



## Research article

# Rapid separation and large-scale synthesis of $\beta$ -FeOOH nanospindles for direct coal liquefaction

Jianping Sheng<sup>a,b</sup>, Murzabek Ispolovich Baikenov<sup>c</sup>, Xiaoyu Liang<sup>b</sup>, Xuehui Rao<sup>b</sup>, Fengyun Ma<sup>b</sup>, Xintai Su<sup>b,\*</sup>, Yi Zhang<sup>a,b,\*\*</sup>

<sup>a</sup> College of Chemistry and Chemical Engineering, Central South University, Changsha 410083, China

<sup>b</sup> Ministry Key Laboratory of Oil and Gas Fine Chemicals, College of Chemistry and Chemical Engineering, Xinjiang University, Urumqi 830046, China

<sup>c</sup> The Department of Chemistry Technology and Oil, Buketov Karaganda State University, Karaganda 100028, Kazakhstan



## ARTICLE INFO

## Article history:

Received 22 December 2016

Received in revised form 15 May 2017

Accepted 15 May 2017

Available online 20 May 2017

## Keywords:

Large-scale synthesis

$\beta$ -FeOOH

Catalysis

Direct coal liquefaction

## ABSTRACT

A rapid separation method for the large-scale synthesis (422 g) of  $\beta$ -FeOOH nanospindles has been achieved via a facile hydrolysis route, including a simple surface-modified process with sodium oleate to improve the dispersivity of  $\beta$ -FeOOH in the direct coal liquefaction (DCL) reaction. The as-prepared (also oleic acid-coated)  $\beta$ -FeOOH exhibited superior catalytic activity toward DCL reaction. The percent of conversion, oil yield, and liquefaction degree with the oleic acid-coated  $\beta$ -FeOOH are 92.6, 73.8, and 80.8%, respectively. This facile separation approach allows large-scale production of nanocatalyst without any centrifugation or filtration process, which will be applicable for future industrial DCL processes.

© 2017 Elsevier B.V. All rights reserved.

## 1. Introduction

The state-of-the-arts for transferring coal to liquid fuels have attracted numerous attempts, due to large reserves of coal and the limited reserves of petroleum [1]. Coal can be converted into liquid fuels and other chemicals through two different routes, usually called “direct coal liquefaction (DCL)” and “indirect coal liquefaction (ICL)”. DCL is one of the thermo-chemical methods to convert coal into liquid fuel with a hydrogenation process in the presence of the catalyst [2,3]. In the process of DCL, catalyst plays an important role in cracking C—C bonds and promoting hydrogen transfer [4,5]. In particular, the use of Fe-based catalysts in DCL has attracted much attention due to their relative efficiency and activity, low-cost and environmentally benign behaviors [3,4,6,7]. The facile preparation, mass synthesis and surface modification of the Fe-based catalysts are therefore a matter of great interest and concern [8,9].

It is known that the particle size, morphology, dispersity and surface state play the key roles on the catalytic properties of catalysts. The decrease of the particle size and enhancement of dispersity has been proved effective methods to improve the catalytic properties for DCL [3,10–12]. Some methodologies have been developed to synthesize

Fe-based nanocatalysts for DCL, such as aerosol technique, [13–15] precipitation method, [16–18] hydrothermal method, [19] and impregnation route process [20–22]. Recently, we have prepared 15 nm-sized  $\text{Fe}_3\text{O}_4$  nanocrystals coated with oleic acid by a thermal decomposition method [10]. The as-synthesized  $\text{Fe}_3\text{O}_4$  exhibited excellent catalytic activity toward coal. However, this kind of strategy usually yield only a few tens of grams and need high temperature and expensive high boiling point solvent, which is difficult to meet the requirement of practical application in DCL.

Inspired by the novel development of Shenhua group in China for preparing an active Fe-based catalyst for DCL [23], we had developed a two-phased solution process to achieve the goal of mass synthesis of  $\text{Fe}_3\text{O}_4$  nanocatalysts (875 g) for DCL [24]. However, the process needs lot of organic solvent, such as toluene and ethanol, which hinder its practical applications. Meanwhile, the Shenhua catalyst is highly dispersed ultra-fine FeOOH loading on coal basis prepared by a impregnation procedure [25,26]. While the dispersivity or lipophilic property of the FeOOH does not meet to the demand for coal liquefaction. The hydrolysis of ferric chloride can obtain a FeOOH colloid sol [27–29]. As a continual work of our previous research, [10,24,27] in this work, we have developed a large-scale synthetic method for  $\beta$ -FeOOH through a one-step hydrolysis method, and the fulvic acid substance was first used as flocculant or precipitant to separate the  $\beta$ -FeOOH from the solution. The DCL experiments indicate that the as-prepared (also oleic acid-coated)  $\beta$ -FeOOH showed a superior catalytic activity. Accordingly, the higher catalytic activity may be attributing to finer particles and higher

\* Corresponding author.

\*\* Correspondence to: Y. Zhang, College of Chemistry and Chemical Engineering, Central South University, Changsha 410083, China.

E-mail addresses: [suxintai827@163.com](mailto:suxintai827@163.com) (X. Su), [yzhangcsu@csu.edu.cn](mailto:yzhangcsu@csu.edu.cn) (Y. Zhang).

dispersion of the catalyst species. Significantly, the current strategy of the large-scale synthesis and fast separation of nanocatalysts display a great potential for practical applications.

## 2. Materials and methods

### 2.1. Materials

All chemicals were analytical and used as starting materials without further purification. The  $\text{FeCl}_3 \cdot 6\text{H}_2\text{O}$  and sodium oleate were obtained from Tianjin Zhiyuan Chemical Reagent Co., Ltd. and Tokyo Chemical Industry Co., Ltd. respectively. The raw coal used in this study is a bitumite from the Xigou mine in Xinjiang, China. This coal sample has the characteristics of high volatile matter ( $V_{\text{daf}}$ ), high vitrinite, low moisture, low ash ( $A_{\text{d}}$ ) and low sulfur which indicate that it is suitable for DCL. Its detailed properties of proximate and ultimate analyses are given in Table 1, which were obtained by GB/T 212-2008 and Elementar Vario Macro, respectively. The expanded uncertainties are estimated 5% and 3% for the proximate analysis and the ultimate analysis, respectively [30]. The Xigou coal sample was ground to a particle size of less than 200 meshes and dried in vacuum at 100 °C for 12 h prior to its utilization in the DCL.

### 2.2. Characterization

The obtained  $\beta\text{-FeOOH}$  and oleic acid-coated  $\beta\text{-FeOOH}$  were characterized by X-ray diffraction (XRD) using a Rigaku D/max-ga X-ray diffractometer with a scanning speed of  $2^\circ \text{ min}^{-1}$  ranging from  $10^\circ$  to  $70^\circ$  with  $\text{Cu K}\alpha$  radiation ( $\lambda = 1.54178 \text{ \AA}$ ). Each sample was tested for three times and the spectra are nearly coincident. The transmission electronic microscopy (TEM) analysis was conducted on a model Hitachi H-600 with an accelerating voltage of 100 kV. Fourier transform infrared (FTIR) spectra were collected with a Bruker EQUINOX55 spectrophotometer in the wave number interval between 4000 and  $400 \text{ cm}^{-1}$ . Samples were pressed into plates after mixed with KCl and analyzed immediately. A back-ground spectrum, collected without KCl and sample, was subtracted from each sample spectrum. The uncertainty and expanded uncertainty are  $0.2\text{--}0.9 \text{ cm}^{-1}$  and  $0.4\text{--}1.8 \text{ cm}^{-1}$ , respectively, for different wavelengths. Each sample was tested with FTIR analyzer three times and the spectra are nearly coincident. The mass fraction of iron in the  $\beta\text{-FeOOH}$  nanospindles was determined by flame atomic absorption spectrophotometry (Hitachi Z-2000) with expanded uncertainty of  $0.02 \text{ mg L}^{-1}$ , after microwave digestion (Milestone ETHOS microwave system). Each sample was read three times to obtain a mean value. Concentration was corrected based on volume of acid used in sample preparation. The weight of oleic acid ligands in the synthesized oleic acid-coated  $\beta\text{-FeOOH}$  was calculated by subtracting the weight of  $\beta\text{-FeOOH}$  from the weight of the oleic acid-coated  $\beta\text{-FeOOH}$ .

### 2.3. Preparation and separation of the $\beta\text{-FeOOH}$ nanospindles

The expanded uncertainty for weight is estimated to 0.02 g. The preparation of  $\beta\text{-FeOOH}$  was carried out according to the method

described previously [27]. And the fulvic acid substance was used first for separating the  $\beta\text{-FeOOH}$ . Typically, 1.08 g of  $\text{FeCl}_3 \cdot 6\text{H}_2\text{O}$  ( $0.004 \text{ mol}$ ) was dissolved into 200 mL of distilled water to form a  $0.02 \text{ mol L}^{-1}$  of  $\text{Fe}^{3+}$  solution. After being stirred for 12 h at 80 °C under reflux, the solution was transformed into an opaque yellow colloidal liquid. Then 7 mL ( $7.0 \text{ g L}^{-1}$ ) of fulvic acid substance dilute solution was added into the resulting yellow colloidal liquid to make the  $\beta\text{-FeOOH}$  nanospindles flocculate. Within ten minutes, the yellow products precipitate in the bottom of the vessel. Then the supernatant fluid was removed and the solid was modified with oleic acid groups by reaction with sodium oleate in the presence of hexane and water.

### 2.4. Primary amplification of lab-scale experiment

To achieve the large-scale preparation of the  $\beta\text{-FeOOH}$  nanospindles, this hydrolysis reaction has been amplified. Firstly, the effects of  $\text{Fe}^{3+}$  concentration (0.02, 0.04, and  $0.06 \text{ mol L}^{-1}$ ) were investigated. The results show that it is still viable when the concentration increase to  $0.04 \text{ mol L}^{-1}$  but higher would be fail (Fig. 4c). So, the subsequent large-scale synthesis was carried out in 2 L of reactor with the highest feasible  $\text{Fe}^{3+}$  concentration ( $0.04 \text{ mol L}^{-1}$ ).

### 2.5. Large-scale preparation

The large-scale synthesis of the  $\beta\text{-FeOOH}$  was carried out in a 150 L autoclave reactor through a forced hydrolysis of  $\text{FeCl}_3$  solutions. The expanded uncertainty for weight and volume are estimated to 0.22 g and 0.56 mL respectively. Typically, 1.62 kg of  $\text{FeCl}_3 \cdot 6\text{H}_2\text{O}$  ( $6.0 \text{ mol}$ ) was completely dissolved into 20 L of distilled water. Then, the  $\text{Fe}^{3+}$  solution was transferred into a 150 L autoclave reactor, followed by adding extra 130 L distilled water. The reaction system was stirred at 80 °C for 12 h. Whereafter, the opaque yellow colloidal liquid was taken out.  $1.5 \text{ L}$  ( $7.0 \text{ g L}^{-1}$ ) of fulvic acid substance dilute solution was added into the resulting slurry to make the  $\beta\text{-FeOOH}$  flocculate and precipitate. Subsequently, the supernatant fluid was removed and the obtained products were modified with oleic acid groups by reaction with sodium oleate in the presence of hexane and water. When the reaction has completed, the upper organic layer containing the oleic acid@ $\beta\text{-FeOOH}$  complexes was separated by a separatory funnel. The final products were kept in a certain amount of tetralin after volatilizing the hexane.

### 2.6. Reaction of DCL

The DCL catalysis performance of the prepared products was evaluated in a common DCL reaction system. And the expanded uncertainty for weight is estimated to 0.02 g. In a typical experiment, 7.43 g of Xigou coal powder, 12.25 g of tetralin (solvent), 0.47 g (3 wt% dry and ash-free (daf) as Fe) of synthesized  $\beta\text{-FeOOH}$  nanospindles (catalyst), and 0.24 g of sulfur (2.0 S/Fe mole ratio) (cocatalyst) were well mixed in a 100 mL of autoclave reactor (Dalian Tongda Reactor Co.). Then, the reactor was sealed and flushed several times with hydrogen followed by pressurizing the system to the initial hydrogen pressure of 7.0 MPa at room temperature and next heated to 435 °C. After stirring at 300 rpm for 60 min, the resulting product was taken out and extracted with n-hexane and tetrahydrofuran (THF) successively in a Soxhlet extractor. The n-hexane-soluble (HS), n-hexane-insoluble but THF-soluble, and THF-insoluble substances were defined as oil and solvent, asphaltene and pre-asphaltene (A + PA) and residue, respectively. The direct liquefactions of Xigou coal with the oleic acid-coated  $\beta\text{-FeOOH}$  and without catalyst were also handled under a similar procedure. The conversion, oil yield and

**Table 1**  
Analyses of the Xigou coal sample.

Proximate analysis (wt%)			Ultimate analysis (wt%, daf)					H/C
$M_{\text{ad}}$	$A_{\text{d}}$	$V_{\text{daf}}$	C	H	$O^a$	N	S	
2.21 (0.11)	3.63 (0.22)	43.92 (2.61)	78.51 (2.35)	5.14 (0.18)	13.92 (2.57)	1.24 (0.04)	0.41 (0.01)	0.7856

<sup>a</sup> Obtained by difference; daf: dry and ash-free base;  $M_{\text{ad}}$ : moisture (air dried base);  $A_{\text{d}}$ : ash (dry base, i.e., moisture free base);  $V_{\text{daf}}$ : volatile matter (dry and ash-free base). The expanded uncertainties are provided in parentheses.

liquefaction degree of coal was calculated using the following equations:

$$\text{Conversion (\%)} = [1 - (W_r - W_{\text{ash}} - W_c) / W_{\text{daf}}] \times 100 \quad (1)$$

$$\text{Oil yield (\%)} = [(W_{\text{HS}} - W_s - W_o) / W_{\text{daf}}] \times 100 \quad (2)$$

$$\text{Liquefaction degree (\%)} = [\text{Oil yield (\%)} + (W_A + W_{\text{PA}}) / W_{\text{daf}}] \times 100 \quad (3)$$

$$\text{Gas yield (\%)} = \text{Conversion (\%)} - \text{Liquefaction degree (\%)} \quad (4)$$

where  $W_{\text{daf}}$  is the dry and ash-free weight of coal;  $W_r$  is the weight of residue;  $W_{\text{ash}}$  is the weight of ash;  $W_c$  is the total weight of  $\beta$ -FeOOH and sulfur;  $W_{\text{HS}}$  is the weight of HS;  $W_s$  is the weight of the solvent (12.25 g of tetralin);  $W_o$  is the weight of oleic acid in the catalysis;  $W_A$  is the weight of asphaltene;  $W_{\text{PA}}$  is the weight of pre-asphaltene. And, all the liquefaction yields presented in this paper were the average values from three experimental runs, the errors between the three runs were within  $\pm 2\%$ .

### 3. Results and discussion

#### 3.1. The separation of the hydrolysate

The homogeneous colloidal solution of  $\beta$ -FeOOH (Fig. 1a) was obtained through a hydrolysis of  $0.04 \text{ mol L}^{-1}$   $\text{FeCl}_3$  solution for 12 h. The homogeneous yellow colloidal solution indicated that the  $\beta$ -FeOOH has a good dispersion and the particle size would be very small. However, the filtration of  $\beta$ -FeOOH from the reaction system is difficult because of their small size and homodisperse, and the products can easily enter the filtrate through the filter paper. For this reason, the centrifugal separation was used to separate the products. Nonetheless, the centrifugal separation still needs to spend 5 min under a rotational speed of 10,000 rpm. An efficient fulvic acid substance flocculant was first to be used to simplify the separation process. After undergoing experiment, we demonstrated that the addition of fulvic acid substance solution can rapidly precipitate the  $\beta$ -FeOOH from the reaction system (shown in Fig. 1b). A possible speculation for flocculation precipitates is as follows. Fulvic acid is a bi-product of humic acid, this biologically complex organic compound comes from the totally decomposed of humic material which is extracted from any material containing well-decomposed organic matter-soil, coal, composts etc. Though to date the molecular structure of fulvic acid is still unclear, but it is sure that the existence of a large amount of  $-\text{OH}$ ,  $-\text{NH}_2$ ,  $-\text{COOH}$ ,  $-\text{SH}$  etc. in fulvic acid [31]. These heteroatoms, with unpaired electrons, in functional groups (N, O, S etc.) can complexation with iron atoms on the

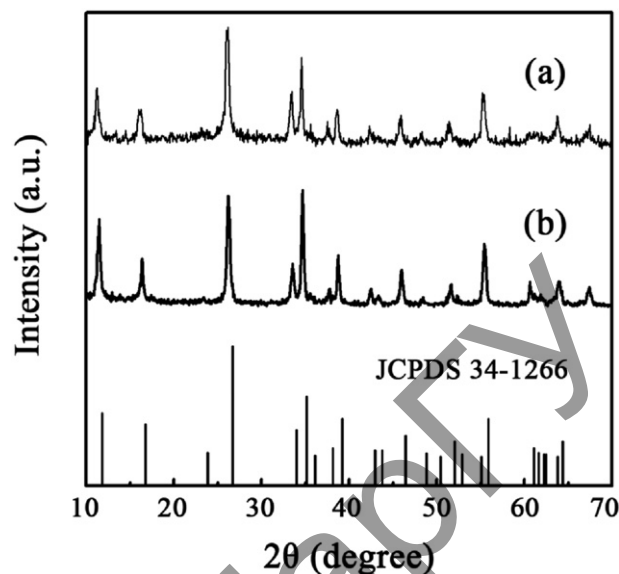


Fig. 2. The XRD images of the  $\beta$ -FeOOH nanospindles obtained (a) without and (b) with use of fulvic acid substance solution.

surface of the nanospindles [32–34]. Then the nanospindles will be taken out of the solution when the fulvic acid flocculation precipitates.

The phase composition and structure of the products were examined by XRD, as shown in Fig. 2. It is obvious that all the diffraction peaks of the two samples can be readily indexed to a tetragonal phase of  $\beta$ -FeOOH phase (JCPDS no. 34-1266). No other peaks of impurities were detected. Fig. 3 presents TEM images of the  $\beta$ -FeOOH obtained with and without use of fulvic acid substance solution. TEM images show that all the two products exhibit a regular spindle shape with diameter of about 20 nm and length of about 100 nm.

From the above data, we can say that the addition of fulvic acid substance solution can rapidly precipitate the  $\beta$ -FeOOH from the reaction system, and the flocculant process has little or no effect on the morphology, size and composition of the products.

#### 3.2. Amplification experiments of preparing $\beta$ -FeOOH nanospindles

To achieve the batch preparation of  $\beta$ -FeOOH, the hydrolysis reaction was enlarged in a planned way.

Firstly, the effect of  $\text{Fe}^{3+}$  concentration in the hydrolysis reaction was investigated. The experiment phenomena and results are listed in Table 2. And some obvious phenomena were observed during these experiments, for example, we can get a homogeneous yellow colloidal solution of  $\beta$ -FeOOH when the  $\text{Fe}^{3+}$  concentration were 0.02 (Fig. 4a) and

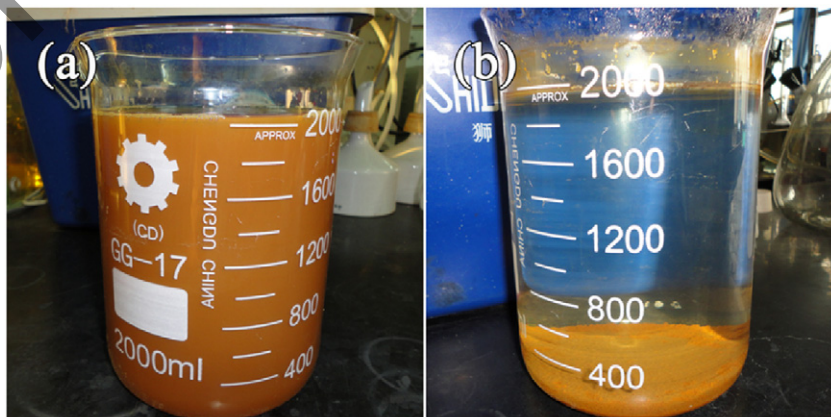


Fig. 1. The photographs of the colloidal solution of  $\beta$ -FeOOH nanospindles (a) before and (b) after use of fulvic acid substance solution.

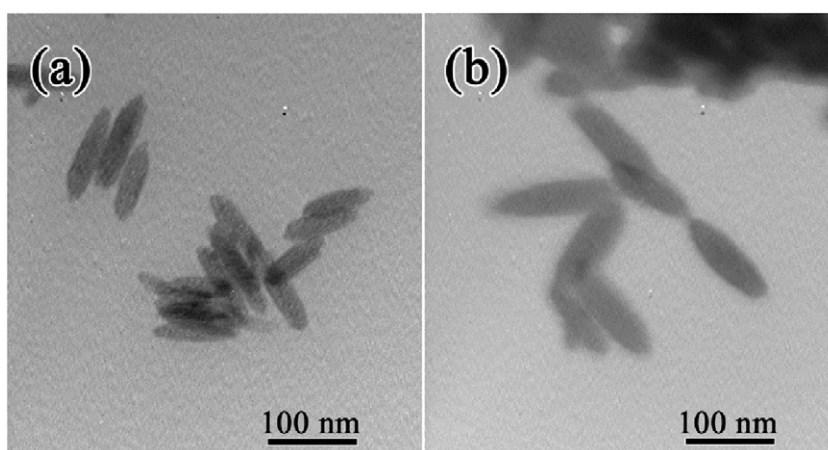


Fig. 3. The TEM images of the  $\beta$ -FeOOH nanospindles obtained (a) without and (b) with use of fulvic acid solution.

$0.04 \text{ mol L}^{-1}$  (Fig. 4b), or a red precipitate of  $\text{Fe}_2\text{O}_3$  when the  $\text{Fe}^{3+}$  concentration increased to  $0.06 \text{ mol L}^{-1}$  (Fig. 4c). This indicated that  $0.04 \text{ mol L}^{-1}$  was the highest concentration of  $\text{Fe}^{3+}$  to obtain  $\beta$ -FeOOH through hydrolysis reaction of  $\text{FeCl}_3$ . Besides, the TEM images (Fig. 5b) also show spindle-shape morphology with slight increase in size. So, the concentration of  $\text{Fe}^{3+}$  was determined as  $0.04 \text{ mol L}^{-1}$  in the following experiments.

Subsequently, the preliminary large-scale synthesis was conducted in a 2 L of reactor, and the obtained products were characterized by XRD (Fig. 4d) and TEM (Fig. 5c). The XRD and TEM patterns show that there are almost no obvious changes on the morphology, size and composition before and after the preliminary large-scale synthesized process. This result indicates that the preliminary large-scale synthesis is feasible.

Lastly, the large-scale synthesis of  $\beta$ -FeOOH was carried out in a 150 L autoclave reactor. And 422 g of  $\beta$ -FeOOH were synthesized at a time. The XRD pattern (Fig. 4e) of the large-scale synthesized products are in good agreement with the characteristic diffractions peaks of the tetragonal phase  $\beta$ -FeOOH, and the TEM images (Fig. 5d) also show a regular spindle shape with diameter of about 20 nm and length of about 100 nm.

### 3.3. The surface modification of the large-scale synthesized $\beta$ -FeOOH nanospindles

Fig. 4f is the typical XRD pattern of the oleic acid-coated  $\beta$ -FeOOH which is in accordance with the tetragonal phase of  $\beta$ -FeOOH. And, the peak intensity of the oleic acid-coated  $\beta$ -FeOOH is obviously lower than the large-scale synthesized hydrophilic  $\beta$ -FeOOH (Fig. 4e); the peak strength decreasing may be caused by the coating of oleic acid ligands on the nanospindle surface.

TEM characterization was applied to investigate the morphology and structure of the oleic acid-coated  $\beta$ -FeOOH. There are not obvious changes on the morphology, size and composition before (Fig. 5d) and after (Fig. 5e) the surface modification process.

FT-IR spectra of the hydrophilic (also oleic acid-coated)  $\beta$ -FeOOH are shown in Fig. 6. Two typical bands at  $854$  and  $674 \text{ cm}^{-1}$  can be ascribed to  $-\text{OH}$  vibrations in  $\beta$ -FeOOH. The adsorption peak at  $413 \text{ cm}^{-1}$  is assigned to  $\text{Fe}-\text{O}$  bending vibrations in  $\beta$ -FeOOH [35]. The occurrence of absorption peaks caused by vibrations of the  $\text{Fe}-\text{O}$  bond and  $-\text{OH}$

bond in the infrared spectrum indicated that the samples must be  $\beta$ -FeOOH. The differences between the FT-IR spectra of hydrophilic  $\beta$ -FeOOH and oleic acid-coated  $\beta$ -FeOOH are obvious. For the oleic acid-coated  $\beta$ -FeOOH (Fig. 6b), the absorption peaks at  $2921$  and  $2851 \text{ cm}^{-1}$  are attributed to the stretching vibration of the  $-\text{CH}_2$  groups in the long alkyl chain of the oleic acid ligands, and the bands at  $1561$  and  $1426 \text{ cm}^{-1}$  are assigned to the asymmetric and symmetric stretching vibrations of  $\text{COO}-$  originating from the carboxylates in the oleic acid ligands [36]. Besides, the adsorption peaks at  $1623 \text{ cm}^{-1}$  in Fig. 3a indicated the presence of structural hydroxyl groups in the hydrophilic  $\beta$ -FeOOH [37]. The above results reveal that the modified  $\beta$ -FeOOH has been coated with hydrophobic oleic acid ligands successfully [24]. In the inset of Fig. 6, it can be observed that the oleic acid-coated  $\beta$ -FeOOH is dispersed in the organic phase, whereas the hydrophilic  $\beta$ -FeOOH is dispersed in the aqueous phase. Based on the results of XRD, TEM and FT-IR, we have reasons to believe that the oleic acid-coated  $\beta$ -FeOOH has successfully obtained hydrophobic surface and it is because of the oleic acid ligands layer coated on the  $\beta$ -FeOOH nanospindles make the  $\beta$ -FeOOH obtain a lipophilic surface, which is beneficial to the DCL process.

### 3.4. Catalytic performance of the samples on DCL

The catalytic activities of the hydrophilic (also oleic acid-coated)  $\beta$ -FeOOH toward the DCL were investigated. As shown in Fig. 7, the

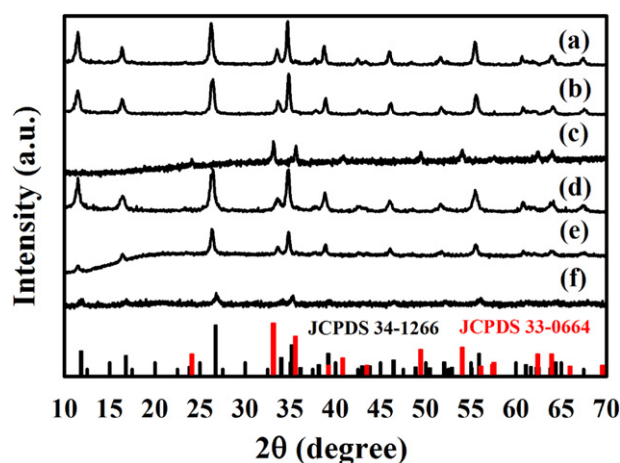


Fig. 4. The XRD images of the products obtained under the synthesis conditions of (a) 0.2 L ( $0.02 \text{ mol L}^{-1}$  of  $\text{Fe}^{3+}$ ), (b) 0.2 L ( $0.04 \text{ mol L}^{-1}$  of  $\text{Fe}^{3+}$ ), (c) 0.2 L ( $0.06 \text{ mol L}^{-1}$  of  $\text{Fe}^{3+}$ ), (d) 2 L ( $0.04 \text{ mol L}^{-1}$  of  $\text{Fe}^{3+}$ ) and (e) 150 L ( $0.04 \text{ mol L}^{-1}$  of  $\text{Fe}^{3+}$ ) of reactor; (f) the oleic acid-coated  $\beta$ -FeOOH.

Table 2

The effect of  $\text{Fe}^{3+}$  concentration on the products.

$\text{Fe}^{3+}/\text{mol L}^{-1}$	0.02	0.04	0.06
Phenomenon	Yellow colloid	Yellow colloid	Red precipitate
Products	$\beta$ -FeOOH	$\beta$ -FeOOH	$\text{Fe}_2\text{O}_3$

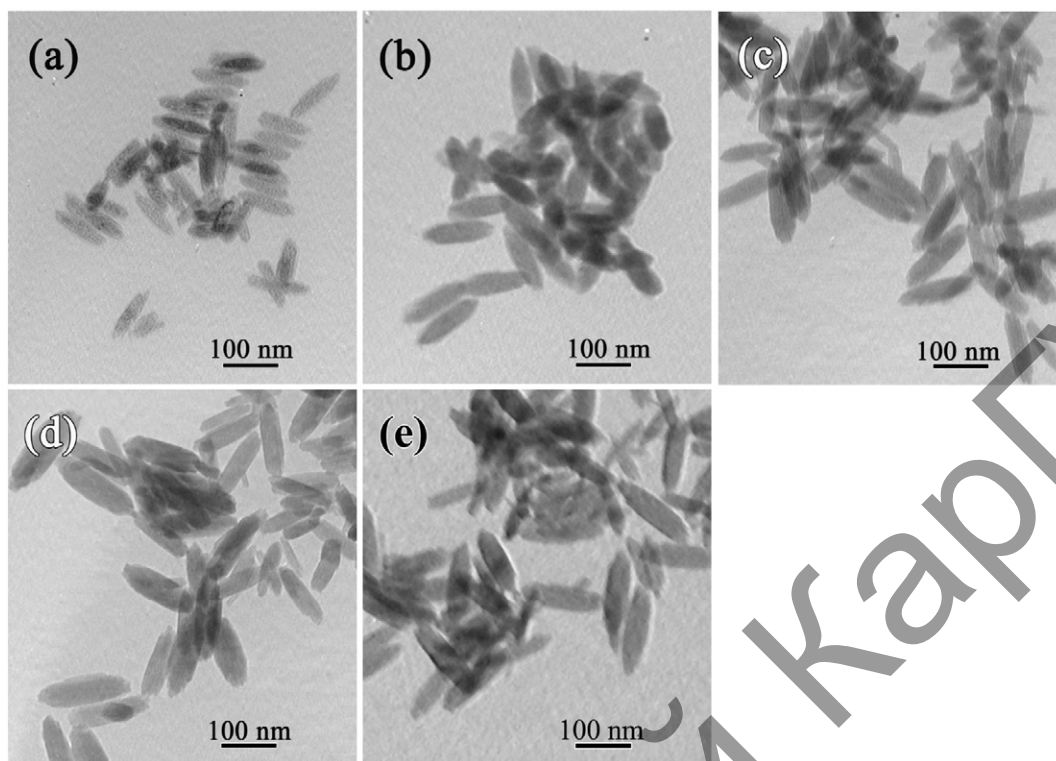


Fig. 5. The TEM images of the products obtained under the synthesis conditions of (a) 0.2 L ( $0.02 \text{ mol L}^{-1}$  of  $\text{Fe}^{3+}$ ), (b) 0.2 L ( $0.04 \text{ mol L}^{-1}$   $\text{Fe}^{3+}$ ), (c) 2 L ( $0.04 \text{ mol L}^{-1}$   $\text{Fe}^{3+}$ ) and (d) 150 L ( $0.04 \text{ mol L}^{-1}$   $\text{Fe}^{3+}$ ) of reactor; (e) the oleic acid-coated  $\beta\text{-FeOOH}$ .

percent of conversion, oil yield, and liquefaction degree in non-catalytic liquefaction reaction are 86.4, 57.7, and 69.0%, respectively, which indicate that the Xigou coal is suitable for DCL under the current conditions. With the addition of 3.0 wt% Fe (based on daf coal) of the hydrophilic  $\beta\text{-FeOOH}$ , the percent of conversion, oil yield, and liquefaction degree reach 88.3, 66.7, and 73.7%, respectively, which demonstrate that the hydrophilic  $\beta\text{-FeOOH}$  have shown a satisfactory performance in DCL. When the oleic acid-coated  $\beta\text{-FeOOH}$  were used in the reaction system, the percent of conversion, oil yield, and liquefaction degree obtained a relatively further increased to 92.6, 73.8, and 80.8%, respectively. To further understand the real reasons of the increased DCL performance, the

yields of other products (asphaltene and pre-asphaltene, residue, and gas) are compared in Fig. 8. From Fig. 8 we can see that the yields of asphaltene and pre-asphaltene, residue and gas are all reduced obviously when the hydrophilic  $\beta\text{-FeOOH}$  is used, and a more significant decrease is obtained upon the use of oleic acid-coated  $\beta\text{-FeOOH}$ . The above data indicate that no matter hydrophilic or oleic acid-coated  $\beta\text{-FeOOH}$  can promote the asphaltene and pre-asphaltene transform more sufficiently to oil species. The inherent catalysis activity of  $\text{FeOOH}$  will be responsible for this phenomenon. And another important reason to the improved DCL performance is the effective inhibition of residue and gas production. That is why the oleic acid-coated  $\beta\text{-FeOOH}$  can further

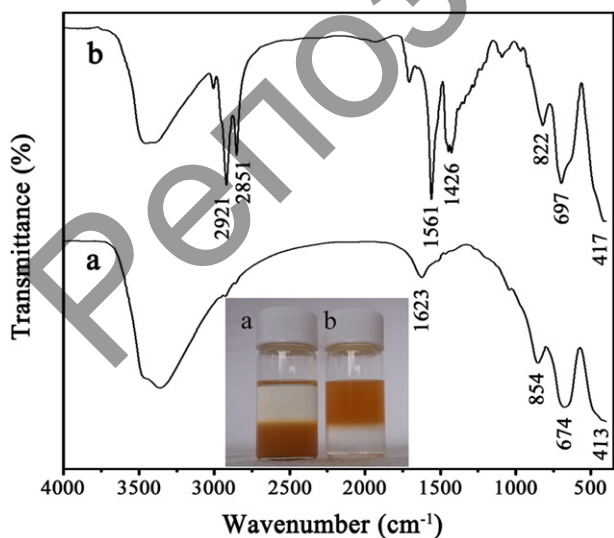


Fig. 6. FT-IR spectra of (a) hydrophilic  $\beta\text{-FeOOH}$  and (b) the oleic acid-coated  $\beta\text{-FeOOH}$ . Inset: Photograph of hydrophilic  $\beta\text{-FeOOH}$  dispersed in water phase (left) and oleic acid-coated  $\beta\text{-FeOOH}$  dispersed in tetralin phase (right).

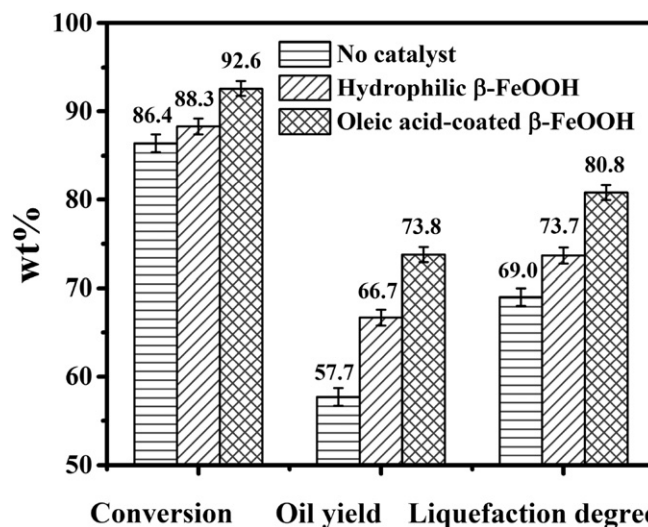


Fig. 7. The percent of conversion, oil yield, and liquefaction degree of the direct liquefaction of Xigou coal with different catalysts.

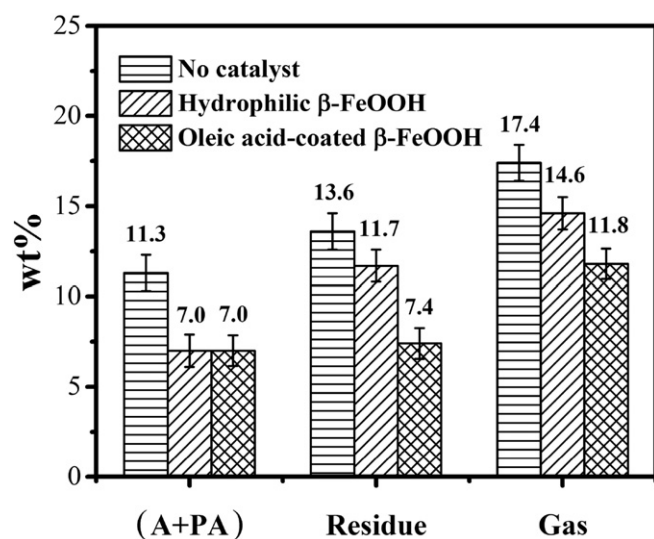


Fig. 8. The percent of asphaltene and pre-asphaltene, residue and gas of the direct liquefaction of Xigou coal with different catalysts.

improve the DCL performance when its asphaltene and pre-asphaltene yield is the same with hydrophilic  $\beta$ -FeOOH.

From our perspective, the inherent catalytic activity, relatively small and uniform morphology and hydrophobic surface are the main reasons for the outstanding catalytic activity of the hydrophilic  $\beta$ -FeOOH and the oleic acid-coated  $\beta$ -FeOOH. Nevertheless, a large amount of active sites of the surface of the hydrophilic  $\beta$ -FeOOH nanospindles will lose impute to the serious agglomeration of catalyst particles in the DCL system. Undoubtedly, the sodium oleate modified hydrophobic  $\beta$ -FeOOH nanospindles won more opportunities to display higher catalytic activity owing to the hydrophobic surface making them adequately dispersion in the DCL system which based on the theory of "similarity and intermiscibility". Besides, the agglomeration of nanoparticles in DCL system can also be prevented with the help of oleic acid on the surface of nanoparticle. The superiority of oleic acid-coated  $\beta$ -FeOOH must be an integrated result of inherent catalytic activity, size, morphology and dispersion. Previous reports have indicated that  $\beta$ -FeOOH is initially transformed into active phase  $\text{Fe}_1-x\text{S}$  when reacting with cocatalyst (S) in the DCL process [38]. Then, adsorption and split of  $\text{H}_2$  molecule will happen on surface of active  $\text{Fe}_1-x\text{S}$ . Finally, the generated hydrogen radical ( $\text{H}\cdot$ ) is transferred to macromolecule of coal and take part in the cracking and stabilization process of coal with the help of hydrogen-donor solvent. The excellent dispersibility in DCL system and relatively large specific surface area make the oleic acid-coated  $\beta$ -FeOOH nanospindle very suitable for the above steps.

#### 4. Conclusions

We developed a facile method to produce  $\beta$ -FeOOH nanospindles with length of about 100 nm and diameter of about 20 nm in large-scale, and also a rapid separation on a large-scale through a one-step hydrolysis process. After a simple two-phase coating method to link oleic acid onto  $\beta$ -FeOOH, the hydrophobic  $\beta$ -FeOOH exhibited an excellent catalytic performance for the DCL. With the oleic acid-coated  $\beta$ -FeOOH, the percent of conversion, oil yield, and liquefaction degree reached to 92.6%, 73.8% and 80.8%, respectively. The synthetic procedure is simple, inexpensive, and scalable for mass production, and the oleic acid-coated  $\beta$ -FeOOH nanocomposites have great potential for industrial applications.

#### Acknowledgements

This work was supported by the National Natural Science Foundation of China (Grant No. 21266031, 51125001, and 51172005).

#### References

- [1] S. Vasireddy, B. Morreale, A. Cugini, C. Song, J.J. Spivey, Clean liquid fuels from direct coal liquefaction: chemistry, catalysis, technological status and challenges, *Energy Environ. Sci.* 4 (2011) 311–345.
- [2] I. Mochida, O. Okuma, S.H. Yoon, Chemicals from direct coal liquefaction, *Chem. Rev.* 114 (2014) 1637–1672.
- [3] H.F. Shui, Z.Y. Cai, C.B. Xu, Recent advances in direct coal liquefaction, *Energies* 3 (2010) 155.
- [4] X. Li, S.X. Hu, L.J. Jin, H.Q. Hu, Role of iron-based catalyst and hydrogen transfer in direct coal liquefaction, *Energy Fuel* 22 (2008) 1126–1129.
- [5] F. Derbyshire, Role of catalysis in coal liquefaction research and development, *Energy Fuel* 3 (1989) 273–277.
- [6] E. Bermejo, T. Becue, C. Lacour, M. Quarton, Synthesis of nanoscaled iron particles from freeze-dried precursors, *Powder Technol.* 94 (1997) 29–34.
- [7] V. Pradhan, D.E. Herrick, J.W. Tierney, I. Wender, Finely dispersed iron, iron-molybdenum, and sulfated iron oxides as catalysts for coprocessing reactions, *Energy Fuel* 5 (1991) 712–720.
- [8] B. Jang, M. Park, O.B. Chae, S. Park, Y. Kim, S.M. Oh, Y.Z. Piao, T. Hyeon, Direct synthesis of self-assembled ferrite/carbon hybrid nanosheets for high performance lithium-ion battery anodes, *J. Am. Chem. Soc.* 134 (2012) 15010–15015.
- [9] L.Q. Wang, X.Z. Li, X.X. Jiang, W.S. Chen, L.S. Hu, M.D. Walle, L. Deng, M.H. Yang, Y.-N. Liu, S.I. Kirin, When protein-based biomimetalization meets hydrothermal synthesis: the nanostructures of the as-prepared materials are independent of the protein types, *Chem. Commun.* 51 (2015) 17076–17079.
- [10] Y.Z. Li, F.Y. Ma, X.T. Su, C. Sun, J.C. Liu, Z.Q. Sun, Y.L. Hou, Synthesis and catalysis of oleic acid-coated  $\text{Fe}_3\text{O}_4$  nanocrystals for direct coal liquefaction, *Catal. Commun.* 26 (2012) 231–234.
- [11] A.V. Cugini, D. Krastman, D.V. Martello, E.F. Frommell, A.W. Wells, G.D. Holder, Effect of catalyst dispersion on coal liquefaction with iron catalysts, *Energy Fuel* 8 (1994) 83–87.
- [12] A.S. Hirschorn, R.B. Wilson, Highly dispersed coal liquefaction catalysts, *Fuel* 71 (1992) 1025–1031.
- [13] R.K. Sharma, J.S. MacFadden, A.H. Stiller, D.B. Dadyburjor, Direct liquefaction of coal using aerosol-generated ferric sulfide based mixed-metal catalysts, *Energy Fuel* 12 (1998) 312–319.
- [14] R.K. Sharma, A.H. Stiller, D.B. Dadyburjor, Effect of preparation conditions on the characterization and activity of aerosol-generated ferric sulfide-based catalysts for direct coal liquefaction, *Energy Fuel* 10 (1996) 757–765.
- [15] R. Bacaud, M. Besson, G. Djega-Mariadassou, Development of a new iron catalyst for the direct liquefaction of coal, *Energy Fuel* 8 (1994) 3–9.
- [16] T. Kaneko, K. Tazawa, N. Okuyama, M. Tamura, K. Shimasaki, Effect of highly dispersed iron catalyst on direct liquefaction of coal, *Fuel* 79 (2000) 263–271.
- [17] J.M. Zhao, Z. Feng, F.E. Huggins, G.P. Huffman, Binary iron oxide catalysts for direct coal liquefaction, *Energy Fuel* 8 (1994) 38–43.
- [18] V.R. Pradhan, J. Hu, J.W. Tierney, I. Wender, Activity and characterization of anion-modified iron(III) oxides as catalysts for direct liquefaction of low pyrite coals, *Energy Fuel* 7 (1993) 446–454.
- [19] F. Derbyshire, T. Hager, Coal liquefaction and catalysis, *Fuel* 73 (1994) 1087–1092.
- [20] S. Methakrup, S. Ngamprasertsith, P. Prasassarakich, Improvement of oil yield and its distribution from coal extraction using sulfide catalysts, *Fuel* 86 (2007) 2485–2490.
- [21] L. Zhang, J.L. Yang, J.S. Zhu, Z.Y. Liu, B.Q. Li, T.D. Hu, B.Z. Dong, Properties and liquefaction activities of ferrous sulfate based catalyst impregnated on two Chinese bituminous coals, *Fuel* 81 (2002) 951–958.
- [22] Z. Liu, J. Yang, J.W. Zondlo, A.H. Stiller, D.B. Dadyburjor, In situ impregnated iron-based catalysts for direct coal liquefaction, *Fuel* 75 (1996) 51–57.
- [23] J. Li, J.L. Yang, Z.Y. Liu, Hydrogenation of heavy liquids from a direct coal liquefaction residue for improved oil yield, *Fuel Process. Technol.* 90 (2009) 490–495.
- [24] Y.Z. Li, F.Y. Ma, X.T. Su, L.J. Shi, B.B. Pan, Z.Q. Sun, Y.L. Hou, Ultra-large-scale synthesis of  $\text{Fe}_3\text{O}_4$  nanoparticles and their application for direct coal liquefaction, *Ind. Eng. Chem. Res.* 53 (2014) 6718–6722.
- [25] W.B. Li, G.P. Shu, K.J. Li, W.D. Huo, S.D. Shi, S.F. Du, P. He, Y. Wang, X. Zhu, CN Patent 200410091152.3 (in Chinese), (2004).
- [26] G.P. Shu, W.B. Li, S.D. Shi, K.J. Li, C.L. Wu, M. Zhou, S.F. Du, W.D. Huo, P. He, CN Patent 03153377.9 (in Chinese), (2003).
- [27] X.H. Rao, X.T. Su, C. Yang, J.D. Wang, X.P. Zhen, D.S. Ling, From spindle-like  $\beta$ -FeOOH nanoparticles to  $\alpha$ - $\text{Fe}_2\text{O}_3$  polyhedral crystals: shape evolution, growth mechanism and gas sensing property, *CrystEngComm* 15 (2013) 7250–7256.
- [28] W. Wang, J.Y. Howe, B.H. Gu, Structure and morphology evolution of hematite ( $\alpha$ - $\text{Fe}_2\text{O}_3$ ) nanoparticles in forced hydrolysis of ferric chloride, *J. Phys. Chem. C* 112 (2008) 9203–9208.
- [29] J.K. Bailey, C.J. Brinker, M.L. Mecartney, Growth mechanisms of iron oxide particles of differing morphologies from the forced hydrolysis of ferric chloride solutions, *J. Colloid Interface Sci.* 157 (1993) 1–13.
- [30] Z.Q. Sun, F.Y. Ma, J. Liao, J.M. Liu, M. Zhong, L.T. Kong, Effects of mechanical activation on the co-liquefaction of Xigou sub-bituminous coal from Xinjiang and Karamay petroleum vacuum residues, *Fuel Process. Technol.* 161 (2017) 139–144.

- [31] R.A. Alvarez-Puebla, C. Valenzuela-Calahorra, J.J. Garrido, Theoretical study on fulvic acid structure, conformation and aggregation: a molecular modelling approach, *Sci. Total Environ.* 358 (2006) 243–254.
- [32] R.A. Saar, J.H. Weber, Fulvic acid: modifier of metal-ion chemistry, *Environ. Sci. Technol.* 16 (1982) 510A–517A.
- [33] K. Murray, P. Linder, Fulvic acids: structure and metal binding, *J. Soil Sci.* 35 (1984) 217–222.
- [34] M. Schnitzer, Reactions between fulvic acid, a soil humic compound and inorganic soil constituents, *Soil Sci. Soc. Am. J.* 33 (1969) 75–81.
- [35] Y.X. Yang, M.L. Liu, H. Zhu, Y.R. Chen, G.J. Mu, X.N. Liu, Y.Q. Jia, Preparation, characterization, magnetic property, and Mössbauer spectra of the  $\beta$ -FeOOH nanoparticles modified by nonionic surfactant, *J. Magn. Mater.* 320 (2008) L132–L136.
- [36] A. Hofmann, S. Thierbach, A. Semisch, A. Hartwig, M. Taupitz, E. Ruhl, C. Graf, Highly monodisperse water-dispersible iron oxide nanoparticles for biomedical applications, *J. Mater. Chem.* 20 (2010) 7842–7853.
- [37] J. Lu, D.R. Chen, X.L. Jiao, Fabrication, characterization, and formation mechanism of hollow spindle-like hematite via a solvothermal process, *J. Colloid Interface Sci.* 303 (2006) 437–443.
- [38] C.L. Zhao, L.C. Zhang, S.K. Cao, R.Q. Jiang, Applications of metals and metal sulphides in catalytic hydrocracking of coal and their related model compounds, *Int. J. Oil Gas Coal Technol.* 12 (2016) 142–161.

Репозиторий КарГУ